Relay Placement of Two-Way Multi-Hop Relay Network with Power Adaptation in a Realistic Shadowing Environment

Namzilp Lertwiram, Gia Khanh Tran, Kei Sakaguchi and Kiyomichi Araki
Graduate School of Science and Engineering, Tokyo Institute of Technology
Ookayama 2-12-1, Meguro, Tokyo, Japan, 152–8552
Email: { namzilp, khanhtg, kei, araki } @mobile.ee.titech.ac.jp

Abstract*—Deployment of relay nodes can enhance the coverage of wireless network in shadowing environments. Recently, MIMO Two-way Multi-hop Network (MTMN) has been introduced as a communication scheme to improve channel capacity of relay networks. Moreover, the strategy of Power Adaptation (PA) has been proposed for MTMN to adjust the Signal-to-Interference plus Noise Ratio (SINR) to achieve the highest performance. However, the studies of MTMN has been based on Rayleigh fading channel model which may be far from the reality since all links in the network are not in the same condition, especially when shadowing is dominant. Moreover, the realization of optimum placements in MTMN for relays in the real shadowing environment is still a left-behind issue. Therefore, this paper aims to investigate the optimum relay placements of MTMN by conducting 3D ray-tracing simulation of propagation channel in a real shadowing environment. Based on the results, the optimum relay placements of MTMN without PA are where relay links do not suffer from shadowing effect. On the contrary, the results show that the optimum placements for MTMN with PA case is different since PA can more efficiently reduce the interference at these locations. In addition, this paper proposed a methodology to estimate the optimum locations for MTMN with PA by using the knowledge of node-to-node signal strength which can be simply obtained in the real environment.

I. Introduction

Nowadays, wireless networking has been gaining attentions since wireless device has the benefits of low cost and ease of installation. For real implementation, however, a wireless link suffers from Non-Line-of-Sight (NLOS) problem, also known as shadowing, when there are obstacles between a pair of transmitter (Tx) and receiver (Rx). Employing relay nodes into the network is an efficient technique to enhance the coverage and also the performance of the network [1]-[2].

Recently, Multi-Input Multi-Output (MIMO) technique has been introduced to improve the spectral efficiency of multi-hop relay networks [3]-[4]. In multi-hop networks, interference from co-channel links, however, is still a problem which degrades the network performance. To overcome this challenge, MIMO Two-way Multi-Hop Network (MTMN) has been proposed as a communication scheme which provides adjacent link interference cancellation and bi-directional communication owing to the benefits of MIMO technology [3]. Although adjacent link interference can be eliminated, the capacity of MTMN is limited by far node interference. Hence, Power Adaptation (PA) for MTMN is proposed in [5] to reduce the strength of overreach interference.

As mentioned, shadowing is a key problem of the implementation in real environments, thus the introduction of relay is needed. However, in previous studies of MTMN, both shadowing and non-shadowing links in the network are assumed to follow Independent Identically Distributed (IID) Rayleigh fading model, which may be far from reality.

Moreover, the optimal relay placements as well as how to verify them is still a left-behind issue, especially when PA is applied in the network. One of our works [6] searched for the optimum relay locations of MTMN by constructing an optimization problem of node arrangement to maximize the end-to-end capacity, however the work is once again based on Rayleigh fading channel assumption and a simple exponential pathloss model. In real scenario, the condition of signal degradation for each links, especially for adjacent links and overreach links in a MTMN, is quite different depending on the existence of shadowing. Such method in [6] is impractical in real environments. Thus, it is necessary to study the optimum relay location in MTMN considering a realistic scenario when shadowing is taken into account.

This paper conducts a 3D ray-tracing simulation of propagation channel for MTMN in a real shadowing environment. A ray-tracing simulator called Wireless Insite [8] providing highly accurate 3D ray searching in building environment is utilized. Based on the simulated propagation results, this paper aims to investigate the following issues.

- By comparing the capacity of MTMN based on 3D ray-tracing model and conventional Rayleigh model, the results show that the end-to-end capacity derived from 3D ray-tracing channels is much higher since overreach interference links strongly suffer from shadowing.
- When PA is not applied, the optimum relay placement is shown to be the location in Line-of-Sight (LOS) of its two adjacent nodes.
- Although when PA is applied, at low Tx power, the optimum relay placement is similar to the case when PA is not applied. However, at high Tx power, the optimum relay placements become locations closer toward the source or the destination nodes where PA can effectively reduce overreach interference even some relay links are allowed to suffer from shadowing.
- Obtaining MIMO channel data of various node locations in real environments is a difficult task for network planner to verify the optimum relay locations in MTMN with PA.

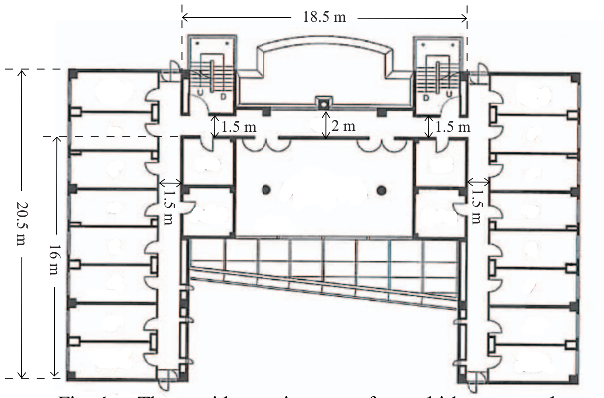

Fig. 1. The corridor environment for multi-hop network.

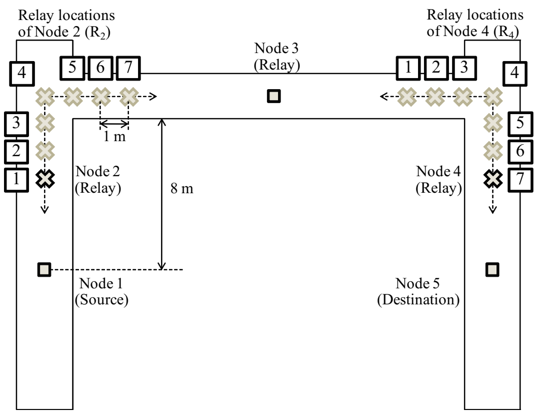

Fig. 2. The multi-hop network topology in corridor environment.

This paper proposes a method to estimate the optimum placement of relay nodes by using only the knowledge of signal strength between nodes.

This paper is organized as follows. The considered environment and propagation model is introduced in Section II and the relay communication schemes used in our analyses are briefly described in Section III. Then, Section IV discusses the analysis results of network performance and optimum relay placements. Then, Section V proposes a novel method to verify the optimum relay placement. Finally, Section VI concludes this paper.

II. Target Environment and Propagation Models

A. Multi-Hop Network Environment and Network Topology

In this paper, we consider a corridor of concrete dormitory [7], as shown in Fig. 1. In this figure, the corridor consists of two straight corridors respectively in the left and right hand side connected by another straight corridor in the middle. The concrete wall along the corridor consists of several wooden doors of private rooms and glass windows. The height of the corridor is 2.4 meter.

In this paper, multi-hop relay network contains 5 transceiver nodes denoted as node 1, 2, 3, 4 and 5, as shown in Fig 2. Source node 1 and destination node 5 are located at the left and right hand side straight corridors where shadowing has a strong effect on the direct wireless link. The other three relay nodes are employed in the network and placed in locations along the shape of corridor. Node 3 is fixed at the center of the middle corridor while node 2 and 4 are located in various locations along two corners of the corridor. The relay location of node 2 and 4 are varied with one meter spacing and their corresponding locations are denoted by the number of 1 to 7 as shown in Fig. 2.

TABLE I
SIMULATION PARAMETERS.

Center frequency	5.06 GHz
Antenna height	2.3 m
Reflection times	8 times
Diffraction times	2 times
Penetration times	4 times

B. Propagation Models

1) 3D Ray-tracing Propagation Model: In this paper, 3D ray-tracing simulator called Wireless Insite [8] is used to generate propagation channel of multi-hop network in the corridor environment since we cannot perform the real measurement in the field. With this simulator, the information of building introduced in the previous subsection can be constructed in three dimensions and the locations of the transceivers can be defined. Once the propagation environment is created, ray-tracing can be started with the simulation parameters described in Table I.

From the simulation, the information of ray paths for each Tx-Rx pair with single antenna is obtained. In this model, the fundamental of array signal processing [9] is applied to reconstruct MIMO channel with 3 transmitter and 3 receiver antennas (3×3 MIMO), $\mathbf{H} \in C^{3\times3}$ by using the knowledge of Angle of Departure/Arrival (AoD/AoA), amplitude, and phase shift of each ray path. The antenna configuration is designed as antenna with half-wavelength spacing linear array antenna.

2) Rayleigh Fading Model (Reference Model): As a reference model, IID Rayleigh fading channel is considered. Generally, MIMO channel can be represented as $\mathbf{H} = \sqrt{\xi}\mathbf{H}_{\text{i.i.d.}}$, where $\mathbf{H}_{\text{i.i.d.}}$ denotes IID Rayleigh fading MIMO channel matrix and ξ denotes channel pathloss. In the reference model, the characteristic of pathloss is based on the empirical pathloss model as, $\xi_{\text{dB}} = -10\alpha\log_{10}(\frac{d}{d_0}) - A$, where d, d_0, α and A respectively denote the node-to-node distance, a reference distance, the pathloss decay exponent, and a constant given by specific model, such as in free space of $A = 20\log_{10}(4\pi d_0/\lambda)$, where λ denotes the signal wavelength. In this paper, the constants of reference distance and pathloss exponent are $d_0 = 1$ m and $\alpha = 3.5$, and the constant $A = 40$ dB.

III. Relay Communication Schemes

In all multi-hop network schemes, all nodes are assumed to have perfect synchronization with perfect knowledge of channel state information of the adjacent nodes.

A. Conventional MIMO Multi-Hop Scheme

The architecture of the conventional MIMO multi-hop scheme is illustrated in Fig. 3a. In this paper, the network

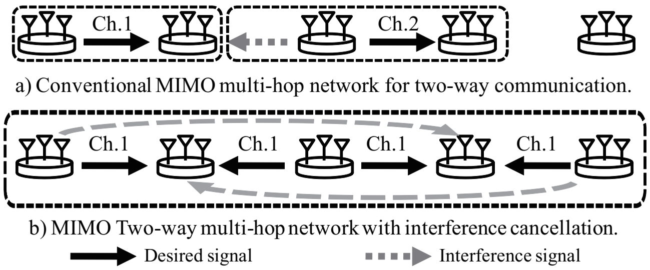

Fig. 3. Conventional MIMO multi-hop and Two-way multi-hop network.

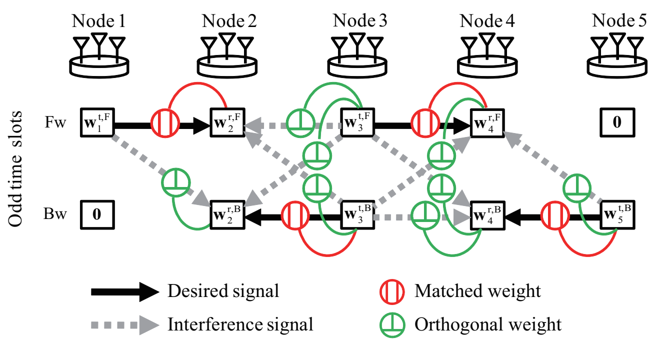

Fig. 4. Flow multiplexing for MIMO two-way multi-hop network.

contains 5 nodes ($N = 5$). There are two states of each node, i.e. Tx and Rx. As shown in Fig. 3a, the conventional MIMO multi-hop scheme needs at least four time slots to perform two-way relaying. Since the communication is in one-way manner, nodes in Rx state are strongly interfered from their adjacent nodes in opposite direction. In order to avoid this interference, two distinct frequencies are assigned for any two adjacent links.

B. MIMO Two-Way Multi-Hop Network Scheme

MTMN differs from the conventional scheme in two aspects. First, with MIMO spatial multiplexing, MTMN allows each Tx node to simultaneously transmit the forward (Fw) and backward (Bw) flows to its following and preceding nodes. Second, MTMN provides adjacent node interference cancellation by joint Tx/Rx array processing. This feature allows all transmission links share the same channel. In comparison to conventional scheme in Fig. 3, the resource of MTMN is less than that in conventional scheme since MTMN needs only single frequency with two time slots to communicate bi-directionally.

In order to achieve Fw/Bw stream multiplexing with adjacent node interference cancellation, each node is equipped with 3 antennas ($M = 3$). Figure 4 shows the details of MTMN in odd time slots. Here, $\mathbf{w}_n^{\text{tF}} \in \mathrm{C}^M$ and $\mathbf{w}_n^{\text{tB}} \in \mathrm{C}^M$ ($n = 1, 3, 5$) are Tx weight vectors for Fw and Bw links at n^{th} node respectively. Similarly, $\mathbf{w}_n^{\text{rF}} \in \mathrm{C}^M$ and $\mathbf{w}_n^{\text{rB}} \in \mathrm{C}^M$ ($n = 2, 4$) are Rx weight vectors for Fw and Bw links at n^{th} node respectively. These vectors in even time slots are also similarly considered. Each weight is assigned to be orthogonal weight to cancel interference signals or matched weight to achieve diversity combining on desired signals. The calculation method of weights are described in [3].

After obtaining weights, the leakage channel gain of each link and each direction can be calculated. Since the multi-hop network consists of $N = 5$ nodes, the number of co-channel links L becomes $L = N - 1 = 4$. In MTMN, each node switches its role as Tx and Rx every time slot. In our system, the set of Fw and Bw links in odd time slots are $I_{\text{o}}^{\text{F}} = \{1, 3\}$ and $I_{\text{o}}^{\text{B}} = \{2, 4\}$ respectively, and those in even time slots are $I_{\text{e}}^{\text{F}} = \{2, 4\}$ and $I_{\text{e}}^{\text{B}} = \{1, 3\}$ respectively. Therefore, the leakage channel gain between the Tx node $\text{T}(j)$ of link j, and the Rx node $\text{R}(i)$ of link i by:

$$g_{i,j} = \mathbf{E}\left[\left|(\mathbf{w}_i^{\text{r,dir}(i)})^H \mathbf{H}_{\text{R}(i),\text{T}(j)} \mathbf{w}_j^{\text{t,dir}(j)}\right|^2\right], \tag{1}$$

where $\text{dir}(i)$ and $\text{dir}(j)$ indicates the direction (Fw or Bw) of link i and link j, and $\mathbf{H}_{\text{R}(i),\text{T}(j)}$ is channel matrix of the link between $\text{T}(j)$ and $\text{R}(i)$ based on the models described in the previous section.

Then channel capacity of link i can be calculated by

$$C_i^{\text{dir}(i)} = \log_2(1 + \bar{\gamma}_i^{\text{dir}(i)}), \tag{2}$$

$$\bar{\gamma}_i^{\text{dir}(i)} = \frac{g_{i,i}p_i}{\sum\limits_{i \neq j} g_{i,j}p_j + n_i}, \tag{3}$$

where $\bar{\gamma}_i^{\text{dir}(i)}$ denotes the average Signal to Interference plus Noise Ratio (SINR) of link i, n_i denotes the noise power of link i and p_i denotes the transmit power of link i. In this case, power adaptation is not applied , so the transmit power of all links are set to be equal.

In multi-hop network, End-to-End capacity is limited at the bottleneck link. Therefore, the network capacity can be calculated by

$$C_{\text{E2E}} = \frac{1}{2}\left(C_{\text{E2E}}^{\text{F}} + C_{\text{E2E}}^{\text{B}}\right) \text{ [bits/s/Hz]}, \tag{4}$$

where $C_{\text{E2E}}^{\text{F}} = \min\limits_{i \in I_{\text{o}}^{\text{F}} \cup I_{\text{e}}^{\text{F}}} \bar{C_i^{\text{F}}}$ and $C_{\text{E2E}}^{\text{B}} = \min\limits_{i \in I_{\text{o}}^{\text{B}} \cup I_{\text{e}}^{\text{B}}} \bar{C_i^{\text{B}}}$ are the End-to-End capacity of Fw and Bw streams.

C. MIMO Two-Way Multi-Hop Network Scheme with Power Adaptation

In this section, PA strategy is employed to adjust the transmission power to increase SINR of the bottleneck link as well as to increase the end-to-end capacity. Here, the proposed Optimum Power Allocation (OPA) scheme in [5] is employed. The following briefly describes the formulation of optimization problem for OPA in MTMN.

The optimization problem of OPA in MTMN is constructed as follows,

$$\begin{aligned} &\underset{\mathbf{p}}{\text{maximize}} && \min_{i = I_{\text{o}}^{\text{dir}(i)}, I_{\text{e}}^{\text{dir}(i)}} \overline{\gamma_i^{\text{dir}(i)}} \\ &\text{subject to} && p_i + p_j \leq p_{\text{max}} \forall i \neq j \text{s.t.} T(i) = T(j), \end{aligned}$$

where $\mathbf{p} = [p_1, ..., p_L]^T$ is the power vector to be optimized. This problem can be solved by the Geometric Programing [10] described in [5]. Finally, the End-to-End capacity of MTMN can be calculated with the optimum power $\mathbf{p}^\star$ obtained from the above convex problem.

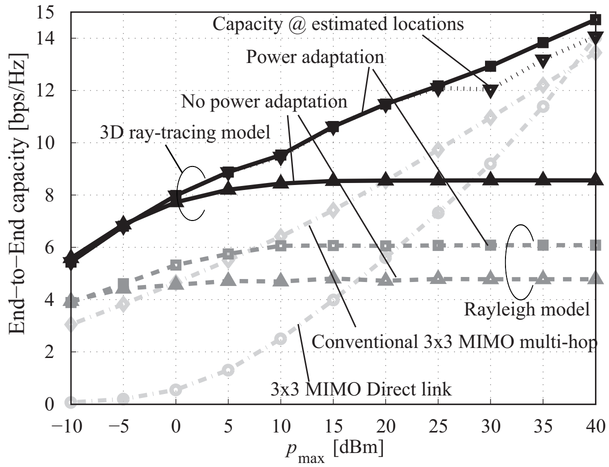

Fig. 5. Comparison of network capacity in different scenarios.

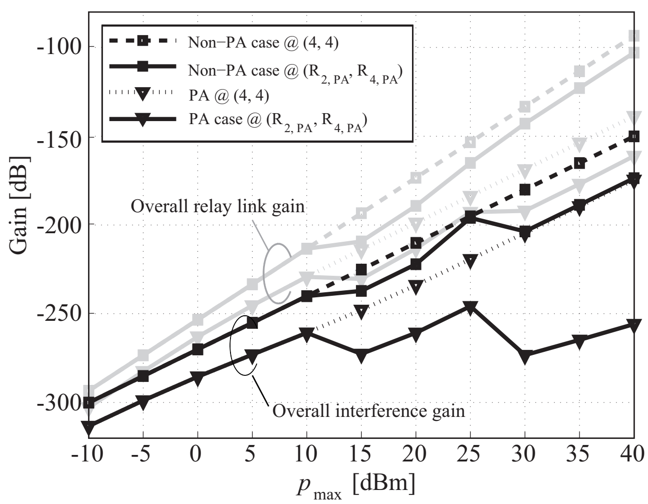

Fig. 6. Characteristic of overall link gain.

IV. Numerical Analysis

In this section, the network capacity of each relaying schemes described in Section III at each pair of relay locations of node 2 and 4 (R_2, R_4) are calculated. Then, the optimum relay locations can be obtained by finding the pair of relay locations of node 2 and 4 that can achieve the maximum network capacity.

A. Capacity Performance Comparison of Multi-Hop Network based on 3-D Ray-Tracing Model

Figure 5 shows the comparison of End-to-End capacity in several relaying schemes at the optimum relay locations shown in Table II with respect to maximum Tx power constraint of each node $p_{\max}$. As shown in the figure, MTMN with PA outperforms the other schemes significantly. Also, when $p_{\max}$ is low, direct transmission extremely suffers from shadowing and conventional MIMO multi-hop with dual channel needs more bandwidth and time slots for two-way communication, so MTMN both with and without can achieve higher capacity than these two schemes. On the contrary, when $p_{\max}$ is high, these two schemes have no interference limitation and channel

TABLE II
Optimum locations (R_2, R_4) in each scenario.

$p_{\max}$ [dBm]	-10	-5 $\sim$ 5	10	15 $\sim$ 20	25	30 $\sim$ 40
No PA(3D)	4, 4	4, 4	4, 4	4, 4	4, 4	4, 4
PA(3D)	4, 4	4, 4	1, 4	1, 4	2, 4	2, 5
PA(Rayleigh)	1, 4	1, 7	1, 7	1, 7	1, 7	1, 7
Estimation	4, 4	4, 4	4, 4	1, 4	1, 4	1, 7

gain can overcome shadowing loss in direct transmission, so capacity of these two schemes approaches to MTMN.

B. Capacity Performance Analysis of MTMN based on 3D Ray-Tracing Model and Rayleigh Model

By comparing the network performance of reference model and 3D ray-tracing model in Fig. 5, the result shows that the performance of the network based on 3-D ray-tracing model is better than the case of theoretical model. Since all links in Rayleigh model are assumed with the same pathloss decay exponent, far node interference is not weakened by strong shadowing effect as that in 3D ray-tracing model. Moreover, Table II shows the optimum relay locations of Rayleigh model in PA case are the locations closest to the source and the destination since overreach interference is weakest due to the length of distance. Therefore, Rayleigh model is not effective when strong effect of shadowing is considered.

C. Optimum Relay Placements of Multi-Hop Network Based on 3-D Ray-Tracing Model

From the results shown in Fig. 5 and the first two rows of Table II, we found that optimum relay locations are always at the corner of the corridor ($(R_2, R_4) = (4, 4)$) in all cases without PA, while the optimum locations of node 2 and 4 become closer to the source and the destination in MTMN with PA when $p_{\max}$ is high. $(R_{2,\text{PA}}, R_{4,\text{PA}})$ is denoted as optimum relay locations when PA is applied. Normally, in a relay network without PA, the most suitable relay placement is where the relay node can properly relay signal from its adjacent nodes without or least blocking from shadowing. However, in MTMN, far node interference is also one factor which affects to the optimum relay placement. In the case of MTMN without PA, signal strength of relay links is a main factor affecting the optimum relay placements while in the case of PA, the power adjustment is used to reduce the interference to improve SINR.

In order to confirm the reason of these optimum relay locations, the characteristics of signal strength of both relay links and interference links are investigated. In order to do so, the overall relay link gain and the overall interference link gain are respectively defined in the following equations,

$$g_{\text{re}} = \prod_{\forall i \in I_{\text{o}}^{\text{F}} \cup I_{\text{e}}^{\text{F}}} \frac{g_{i,i}}{N_{\text{re}}^{\text{F}}} + \prod_{\forall i \in I_{\text{o}}^{\text{B}} \cup I_{\text{e}}^{\text{B}}} \frac{g_{i,i}}{N_{\text{re}}^{\text{B}}} \tag{5}$$

$$g_{\text{if}} = \prod_{\forall i \in I_{\text{o}}^{\text{F}} \cup I_{\text{e}}^{\text{F}}} \left(\sum_{i \neq j} \frac{g_{i,j}}{N_{\text{if}}^{\text{F}}} \right) + \prod_{\forall i \in I_{\text{o}}^{\text{B}} \cup I_{\text{e}}^{\text{B}}} \left(\sum_{i \neq j} \frac{g_{i,j}}{N_{\text{if}}^{\text{B}}} \right), \tag{6}$$

where N_{re}^{F} and N_{re}^{B} denote the number of all relay links in $I_{\text{o}}^{\text{F}} \cup I_{\text{e}}^{\text{F}}$ and $I_{\text{o}}^{\text{B}} \cup I_{\text{e}}^{\text{B}}$ respectively, and N_{if}^{F} and N_{if}^{B} denote the number of relay links in $\{i \in I_{\rm o}^{\rm F} \cup I_{\rm e}^{\rm F} \mid \sum_{i \neq j} g_{i,j} \neq 0\}$ and $\{i \in I_{\rm o}^{\rm B} \cup I_{\rm e}^{\rm B} \mid \sum_{i \neq j} g_{i,j} \neq 0\}$ respectively. In these equations, the gain of each link is normalized with the number of existing links for the fair comparison.

Figure 6 shows the characteristic of the network interference gain and relay gain by changing maximum power constraint when $(R_2, R_4) = (4, 4)$ (at the corners) and $(R_2, R_4) = (R_{2,\rm PA}, R_{4,\rm PA})$ (at the optimum placement in PA case). Comparing the interference of MTMN with and without PA (black lines), power adjustment reduces the entire network interference. Interestingly, the reduction is obvious at the optimum relay placements while the relay link gain (gray lines) at location $(R_{2,\rm PA}, R_{4,\rm PA})$ does not differ much from that of location $(4, 4)$. This can imply that the optimum relay placement is a place where interference is adjusted to be lower. On the other hand, in the case of non-PA, the capacity is implied to be interference limited and the optimum placement is dominated by the signal strength of relay links.

V. Relay Placement Estimation Methodology

As discussed in the previous section, the optimum relay location when PA is applied depends on the adjustment of overreach interference. The Tx power adjustment normally has its effect mainly on two factors i.e. the relay link gain and the interference gain which affects the optimum placements. However, MIMO channel is difficult to obtain for network planning in the real environment. This section proposes a method to estimate the optimum relay locations in the network by using the knowledge of node-to-node pathloss which is simpler to verify.

From the ray-tracing simulator, the information of all node-to-node pathloss can be obtained. Pathloss between the Tx node T(j) of link j, and the Rx node R(i) of link i is denoted as $\xi_{i,j}$. The proposed method is adapted from the calculation of power adaptation described in section III. The following paragraph explains the process of this method.

1) For all locations of R_2 and R_4,
   - Consider Fw links, equivalent SINR of link i in Fw direction becomes $\rho_i^F(R_2, R_4) = \frac{p_i \xi_{i,i}}{\sum_{i \neq j} p_j \xi_{i,j} + n_i}$. Bw links can be similarly considered.
   - Since the network is limited by the SINR of the bottleneck link, the optimum power can be obtained by the following convex problem.

$$\begin{array}{ll} \underset{\mathbf{P}}{\text{maximize}} & \min_{i = I_{\rm o}^{\rm dir(i)}, I_{\rm e}^{\rm dir(i)}} \rho_i^{\rm dir(i)}(R_2, R_4) \\ \text{subject to} & p_i + p_j \leq p_{\max} \forall i \neq j \text{s.t.} T(i) = T(j). \end{array}$$

     This problem is solved by GP as described in [10].
   - Find the summation of the minimum SINR of both directions as,

$$\rho_{\min}(R_2, R_4) = \sum_{\rm dir = F,B} \min_{i \in I_{\rm o}^{\rm dir(i)} \cup I_{\rm e}^{\rm dir(i)}} \rho_i^{\rm dir(i)}(R_2, R_4).$$

2) Obtain the optimum relay locations by $(R_{2,opt}, R_{4,opt}) = \arg_{R_2, R_4} \max \rho_{\min}(R_2, R_4)$

By the methodology above, the estimated locations is shown in Table II by changing the maximum power constraint. The real network capacity at the estimated locations is plotted in Fig. 5. As shown in Table II, the estimated locations are the same with the optimum locations when $p_{\max}$ is low or relay link gain has dominant effect. When $p_{\max}$ is high, the capacity at the estimated locations is a little bit lower than the capacity at optimum locations around 6% at maximum. However, the estimated locations are still in the same straight corridor. Therefore, the optimum relay location can be roughly estimated with the proposed method.

VI. Conclusion

This paper investigated MTMN in a real shadowing environment. The result confirmed that Rayleigh fading is not an appropriate assumption for evaluating network performance in real scenario with the existence of shadowing. Moreover, overreach interference limits the network performance especially when PA is not applied. The optimum relay placements in all schemes without PA is shown to be where relay links do not suffer from shadowing. Situation is different when PA is applied since PA provides obvious reduction of interference at these locations. Finally, with the method for verifying optimum relay placements for MTMN with PA, the network planner can roughly estimate the placements where network can obtain the performance close to the real optimum relay placements by using the knowledge of node-to-node signal strength.

References

[1] M. Hasna and M. Alouini, "End-to-end performance of transmission systems with relays over Rayleigh fading channels," *IEEE Trans. Wireless Commun.*, vol.2, pp.1126–1131, Nov., 2003.

[2] J. Boyer, D.D. Falconer and H. Yanikomeroglu, "Multihop diversity in wireless relaying channels," *IEEE Trans. Commu.*, vol.52, no.10, pp.1820–1830 , Oct., 2004

[3] F. Ono and K. Sakaguchi, "MIMO spatial spectrum sharing for high efficiency mesh network," *IEICE Trans. Commun.*, vol.E91-B, pp.62–69, Jan., 2008.

[4] D. Gunduz, A. Goldsmith and H. Poor, "MIMO two-way relay channel: Diversity-multiplexing tradeoff analysis," *Proc. Asilomar Conf. on Signals, Systems and Computers*, 2008.

[5] J. Lee, G.K. Tran, K. Sakaguchi and K. Araki, "Effect of power allocation schemes on MIMO two-way multi-hop network," *IEICE Trans. Commun.*, vol.E93-B, pp.3362–3370, Dec., 2010.

[6] R. Ramamonjison, J. Lee, K. Sakaguchi and K. Araki, "Routing and power allocation in MIMO two-way multi-hop networks: A new cross-layer approach to mitigate interference," *Proc. IEEE Conf. Globcom 2010*, June., 2010.

[7] K. Baba, "Data file of architectural design and details: [37] Organization residences and dormitory (In Japanese)," ISBN 0288-4267, *Kenchiku Shiryo Kenkyusha*, 2ed., 1994.

[8] *http://www.remcom.com/wireless-insite*

[9] D. G. Manolakis, V. K. Ingle, S. M. Kogon, "Statistical and Adaptive Signal Processing," ISBN 1-58053-610-7, *Artech House, Inc*, 2005.

[10] C. Mung, "Geometric programming for communication systems," *Now Publishers*, 2005.